An Iterative Algorithm for Accurate Estimation of Power System Forced Oscillation Parameters

Luke Dosiek and Sanjay Hosur
Department of Electrical, Computer, and Biomedical Engineering
Union College
Schenectady, NY 12309
Emails: dosiekl@union.edu, hosurs@union.edu

***Abstract*—This paper proposes an iterative method of estimating power system forced oscillation (FO) amplitude, frequency, phase, and start/stop times from measured data. It combines three algorithms with favorable asymptotic statistical properties: a periodogram-based iterative frequency estimator, a Discrete-Time Fourier Transform (DTFT)-based method of estimating amplitude and phase, and a changepoint detection (CPD) method for estimating the FO start and stop samples. Each of these have been shown in the literature to be approximate maximum likelihood estimators (MLE), meaning that for large enough sample size or signal-to-noise ratio (SNR), they can be unbiased and reach the Cramer-Rao Lower Bound in variance. The proposed method is shown through Monte Carlo simulations of a low-order model of the Western Electricity Coordinating Council (WECC) power system to achieve statistical efficiency for low SNR values. The proposed method is validated with data measured from the January 11, 2019 US Eastern Interconnection (EI) FO event. It is shown to accurately extract the FO parameters and remove electromechanical mode meter bias, even with a time-varying FO amplitude.**

I. Introduction

Accurately estimating forced oscillation (FO) parameters from measured power system outputs is important when one is attempting to characterize the system-wide shape of the FO response, localize the source of the FO, or perform electromechanical mode estimation in the presence of FOs. This is especially true with the ongoing increase in inverter-based resources and microgrids seen in the modern power system [1]. The mode estimation problem can be troublesome if FOs are not handled correctly; indeed a mode meter can model a FO as a system mode with nearly 0% damping and can trigger false alarms of system instability [2]–[7].

A recent example of such a situation occurred on January 11, 2019 in the United States Eastern Interconnection (EI) where a large 0.25-Hz FO was observed from 08:44:40 to 09:02:26 UTC [8]. Originating from a failed turbine controller on a single generator in Florida, the FO was seen throughout the entire EI due to the close proximity of its frequency to that of a major interarea electromechanical mode. As described in [8], while reliability coordinators (RCs) were quickly aware of the event due to data-driven wide-area situational awareness (WASA) tools, a lack of information led to mischaracterization of the FO.

This material is based upon work supported by the National Science Foundation under Grant No. 1944689

Thus, it is of great importance that FO parameters be accurately estimated in order for WASA tools such as mode meters to provide RCs the best possible picture of the state of the grid. This paper presents an iterative algorithm for estimating FO parameters. It combines a statistically efficient frequency estimator from [9] with the Discrete-Time Fourier Transform (DTFT) to estimate amplitude and phase, and utilizes the changepoint detection (CPD) method from [10] to estimate the FO start/stop times. The proposed method is characterized using Monte Carlo simulations and validated using data from the January 2019 EI event.

The paper is organized as follows. Section II provides reviews the linear modeling of power systems under FO conditions along with parameter estimation techniques and performance assessment. Section III introduces the proposed algorithm. Simulation results are shown in Section IV, while the EI event is covered in Section V. Finally, Section VI provides concluding remarks and future research directions.

II. Background

A. Model Definitions

Under small signal conditions, power systems experiencing forced oscillations may be modeled as an autoregressive moving average with exogenous input (ARMAX) system from the point of view of lowpass filtered and detrended phasor measurement unit (PMU) data [6]. Measured system output $y[k]$ can be expressed as

$$y[k] = \frac{C(q)}{A(q)}e[k] + \frac{B(q)}{A(q)}u[k] = x[k] + s[k] \tag{1}$$

where input $e[k]$ is Gaussian White Noise (GWN) filtered by $C(q)/A(q)$ to create ARMA process $x[k]$ and periodic input $u[k]$ is filtered by $B(q)/A(q)$ to create FO $s[k]$:

$$x[k] = \frac{C(q)}{A(q)}e[k] \tag{2}$$

$$s[k] = \frac{B(q)}{A(q)}u[k] \tag{3}$$

Note that $A(q)$, $B(q)$ and $C(q)$ are the AR, X, and MA polynomials in delay operator q such that $q^{-n}y[k] = y[k-n]$,

and a total of N samples of $y[k]$ are collected at a rate of f_s samples per second. Input $u[k]$ is defined as

$$u[k] = \sum_{i=1}^{p} A_i \cos\left(2\pi \frac{f_i}{f_s} k + \theta_i\right) I_{\epsilon_i,\eta_i}[k] \tag{4}$$

where A_i, f_i and θ_i are the amplitude, frequency (Hz) and phase of the i^{th} input cosine, and indicator function I defines the FO starting sample ϵ_i and ending sample η_i by

$$I_{\epsilon_i,\eta_i}[k] = \begin{cases} 1, & \epsilon_i \leq k \leq \eta_i \\ 0, & \text{else} \end{cases} \tag{5}$$

The FO that is actually observed in the system output is $s[k]$, which will contain the same frequencies as $u[k]$ but will in general have different amplitudes and phases. Additionally, while $u[k]$ is modeled as having abrupt starts and stops via the indicator function, $s[k]$ will start and stop with transients according to the system response. For the remainder of this paper, the subscripts on the parameters in (4) are dropped and it is assumed that $u[k]$ is comprised of a single sinusoid ($p = 1$). The methods presented here can easily be extended to $p > 1$.

B. Parameter Estimation

In [11], the problem of estimating the amplitude, frequency, and phase of a real cosine in noise is heavily studied. It is shown that if frequency f is neither near 0 nor the Nyquist rate, the Discrete-Time Fourier Transform (DTFT) of $y[k]$,

$$Y(f) = \sum_{n=0}^{N-1} y[n] e^{-j2\pi \frac{f}{f_s} n} \tag{6}$$

can be used to provide accurate estimates of FO amplitude, frequency and phase. In particular, the approximate Maximum Likelihood Estimator (MLE) of frequency is found by maximizing the periodogram

$$\hat{f} = \underset{f}{\operatorname{argmax}} \frac{1}{N} |Y(f)|^2 \tag{7}$$

and the approximate MLEs for amplitude and phase are found by evaluating the DTFT at the estimated frequency:

$$\hat{A} = \frac{2}{N} |Y(\hat{f}_o)| \tag{8}$$

$$\hat{\theta} = \underline{/Y(\hat{f}_o)} \tag{9}$$

Note that calculating (7) is not straightforward. A course estimate may be obtained with the Discrete Fourier Transform (DFT or FFT), which may then be refined using any number of methods in the literature, e.g., [9], [12]–[14]. However, many of these methods are biased due to interference from the sidelobes of $-f$ or show heavy dependence upon initial phase θ. Here, the method of [9] is used, which iteratively refines an interpolated FFT of $y[k]$ that has had its negative $\hat{f}$ component removed. It is shown in [9] to be asymptotically unbiased and reaches the CRLB while being insensitive to variations in θ. See [9] for implementation details.

The estimation of the FO start and stop samples ϵ and η was first addressed in the context of power systems in [15]. In [10], an approach based on the MLE for CPD given in [16] was implemented using a linear programming scheme. While more computationally intensive than that of [15], the CPD approach was shown to significantly improve estimation accuracy, and was the method implemented in this paper. Note that the CPD approach to estimating ϵ and η requires an estimate of the FO frequency. Also note from (8) and (9), that the estimates of A and θ, while easy to calculate, also depend upon $\hat{f}$. Thus, starting with a high quality implementation of (7) is *paramount*.

C. Estimation Assessment

In order to assess the quality of the FO parameter estimators, one must consider both accuracy and precision. In the simulation setting, Monte Carlo trials may be utilized whereby a system is simulated hundreds of times, each with an independent random input. FO parameters are estimated from each of the outputs, and accuracy may be assessed by comparing the means of the parameter estimates to the true values. An unbiased estimate should on average converge to the true value.

To assess precision, the variance of the estimates may be compared to the Cramer-Rao Lower Bound (CRLB), which defines the minimum achievable variance for any unbiased estimator. The variance of a statistically efficient estimator should on average converge to the CRLB. Note that if an estimator is biased, it may achieve variance lower than the CRLB. For A, f, and θ, the CRLB are well-known for the cosine-in-GWN case (see [11] for example). In power system FO applications, however, the cosine is in colored noise; specifically an ARMA process. In [17], [18], expressions for the CRLB have been derived. The CRLB on FO start/stop samples ϵ and η has, to the best of the authors' knowledge, never been derived and is a subject of ongoing work.

III. Iterative Estimation of FO Parameters

An important detail surrounding the estimation of A, f, and θ that methods described by (7) - (9) assume the FO is present throughout the entire data set. Indeed, when $y[k]$ contains some length of ARMA process noise before and/or after the FO, issues arise that can reduce the performance of the estimators. Specifically, $\hat{A}$ will be biased low since (8) is scaled by the length of $y[k]$, not the length of the portion of the data record where the FO is present. More generally, as the FO length $\eta - \epsilon$ gets smaller relative to N, the SNR between the FO and ARMA noise drops in kind, which will result in a overall degradation of estimator performance.

This paper proposes the following algorithm to address the issue at hand. As seen in Algorithm 1, the frequency estimator is abbreviated "SD" after the author of [9], the amplitude and phase estimator is named "DTFT" due to its use of the Discrete-Time Fourier Transform, and the start/stop sample estimator is named "CPD" for its use of changepoint detection.

The superscripts indicate iteration number of a particular estimate.

The procedure starts with the FO detection scheme from [19], which also provides a course frequency estimate, $\hat{f}^{(o)}$. Once detected, the FO frequency estimate is passed to the algorithm along with $y[k]$ and parameter Q, the number of iterations to perform. FO amplitude and phase are initialized as 1 and 0, and the starting and ending samples are initialized as 0 and $N-1$.

The initial frequency estimate $\hat{f}^{(1)}$ is found by refining $\hat{f}^{(o)}$ with SD. The initial amplitude and phase estimates are found using the DTFT and $\hat{f}^{(1)}$, and the initial start/stop samples are estimated using CPD with $\hat{A}^{(1)}$, $\hat{f}^{(1)}$, and $\hat{\theta}^{(1)}$. Note that the entire dataset $y[k]$ is used for this initial round of estimates.

For $i > 1$, the initial estimates are refined $Q-1$ times, where $\hat{A}^{(i)}$, $\hat{f}^{(i)}$, and $\hat{\theta}^{(i)}$ are found using he window of data where the FO is present approximately throughout, i.e., $y[k]$ from samples $\hat{\epsilon}^{(i-1)}$ to $\hat{\eta}^{(i-1)}$. In contrast, the FO start/stop samples are refined using all of $y[k]$ in order to ensure the previous start/stop estimates didn't exclude portions of the FO.

Algorithm 1 Iterative Estimation of FO Parameters

Input: $y[k]$, $\hat{f}^{(o)}$, and Q
Initialize: $\hat{A}^{(o)}$=1, $\hat{\theta}^{(o)}$=0, $\hat{\epsilon}^{(o)}$=0, and $\hat{\eta}^{(o)}$=$N-1$
Output: $\hat{A}$, $\hat{f}$, $\hat{\theta}$, $\hat{\epsilon}$, and $\hat{\eta}$

1: **for** $i = 1$ to Q **do**
2: $\quad \hat{f}^{(i)} = \text{SD}\left(y\left[\hat{\epsilon}^{(i-1)} : \hat{\eta}^{(i-1)}\right], \hat{f}^{(i-1)}\right)$
3: $\quad \left[\hat{A}^{(i)}, \hat{\theta}^{(i)}\right] = \text{DTFT}\left(y\left[\hat{\epsilon}^{(i-1)} : \hat{\eta}^{(i-1)}\right], \hat{f}^{(i)}\right)$
4: $\quad \left[\hat{\epsilon}^{(i)}, \hat{\eta}^{(i)}\right] = \text{CPD}\left(y[0 : N-1], \hat{A}^{(i)}, \hat{f}^{i)}, \hat{\theta}^{(i)}\right)$
5: **end for**
6: **return** $\left[\hat{A}^{(Q)}, \hat{f}^{(Q)}, \hat{\theta}^{(Q)}, \hat{\epsilon}^{(Q)}, \hat{\eta}^{(Q)}\right]$

IV. Simulation Results

To assess the performance of the algorithm, a 17^{th} order ARMA approximation of the minniWECC model of the Western Electricity Coordinating Council (WECC) power system was used. Developed in [20], its output approximates a voltage angle difference where the the "North-South B" (NSB) interarea mode of 0.372 Hz and 4.67 % damping is especially observable in the minniWECC. The ARMA model takes into account the detrending and downsampling typically performed on measured PMU data, resulting in a comparatively low-order representation of the minniWECC sampled at 3 samples-per-second. See [20] for more details on the AMRA approximation and [21] for details on the minniWECC.

Ambient power system and FO data were simulated by filtering GWN and a cosine, respectively, through the ARMA model to create 30 minutes of data with the FO present for the middle 15 minutes. The FO in the output had an amplitude of 1, a phase of $\pi/8$, and a frequency that was identical to that of the NSB mode, 0.372 Hz. The variance of the GWN was varied to create FO-to-ambient-data SNRs ranging from -5 to 20 dB, and 300 Monte Carlo simulations of each SNR case were created. Note these results were obtained with $Q = 2$ in Algorithm 1. That is, no additional accuracy was gained with further iterations in the refinement step.

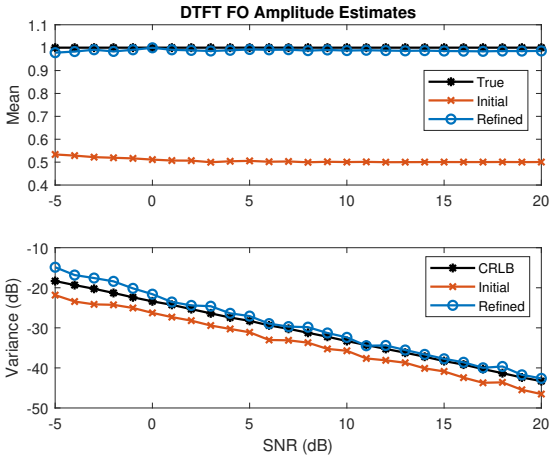

Fig. 1. Initial and refined estimates of FO amplitude from approximate minniWECC model.

In Fig. 1, the amplitude biasing discussed above is apparent. These results are to be expected, since the FO is present for half the data record so a DTFT-based estimator should estimate the FO with half of the true amplitude. The refined estimates are excellent, showing little bias, and variance that reaches the CRLB. The estimates of frequency and phase are shown in Figs. 2 and Fig. 3 demonstrate a stark improvement between the initial and refined estimates, with the mean and variance converging to the true value and CRLB, respectively.

The FO start and stop samples also demonstrated an improvement during the refinement process with both nearly reaching the true values, as seen in Fig. 4. With the CRLB unavailable, the variance may only be compared in a before-and-after refinement sense. Although a small improvement was observed, the variance of the initial and refined estimates was very small across all SNR, and so are omitted due to space constraints.

V. US Eastern Interconnection Results

The proposed algorithm was applied with Q=2 to the January 2019 FO event discussed in Section I. The top of Fig. 5 shows frequency measurements taken at Union College in Schenectady, NY during the event, while the bottom shows the detrended and downsampled version.

The FO parameters were estimated using the proposed algorithm on 40 minutes of data that contained the FO in the middle. Note the SNR here was estimated to be 10.8 dB (see below for details). Similar to the simulation results, the FO amplitude estimates demonstrated the biggest change, going from an initial value of 2.6 mHz up to 5.9 mHz after refinement, while the frequency and phase estimates showed minor adjustment, going from 0.25 Hz and -1.76 rad to 0.25001 Hz and -1.79 rad. The estimated starting and ending samples did not change in the refinement stage, and

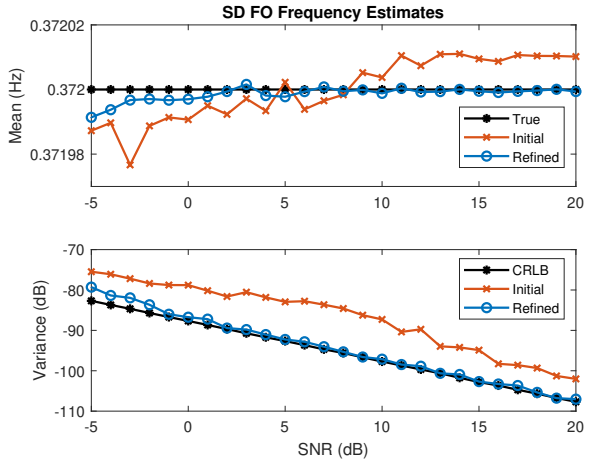

Fig. 2. Initial and refined estimates of FO frequency from approximate minniWECC model.

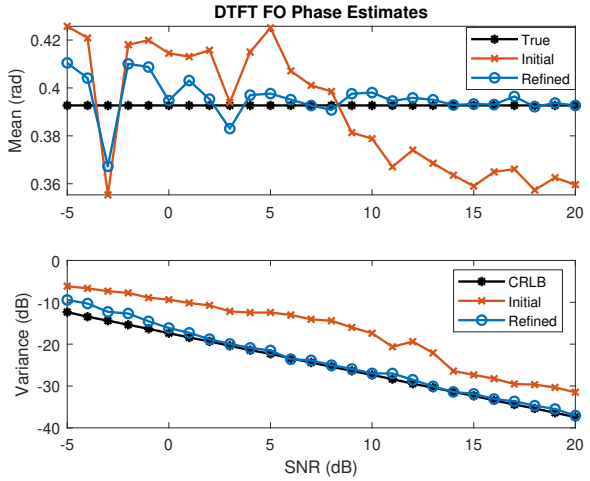

Fig. 3. Initial and refined estimates of FO phase from approximate minniWECC model.

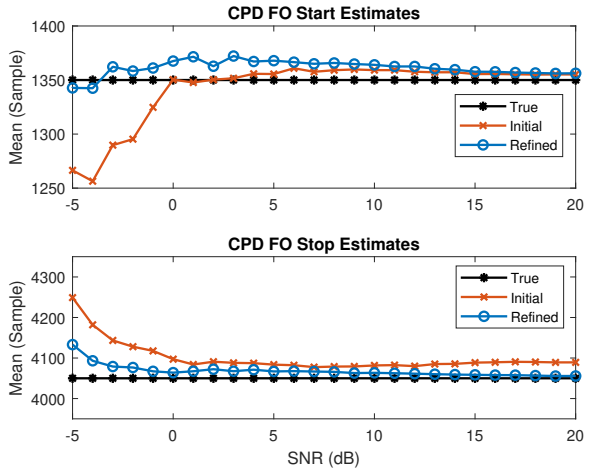

Fig. 4. Initial and refined estimates of FO starting and stopping samples from approximate minniWECC model.

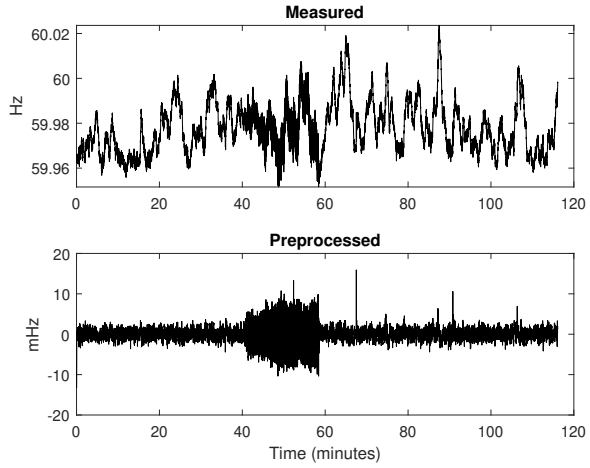

Fig. 5. January 11, 2019 EI FO event measured at Union College (top) and preprocessed (bottom).

were found to be 3274 and 8520, respectively. Note that the timestamps given in [8] correspond to samples 3228 and 8558. It was observed that the algorithm detected neither the initial low-amplitude portion of the onset transient nor the low-amplitude end of the offset transient. Accounting for this is a subject of ongoing work.

Next, a mode meter study was conducted. The data were analyzed by the LS-ARMA mode meter algorithm, which assumes that $y[k]$ is an ARMA process with no FO present [5]. Three data sets were used, each 40 minutes in duration, with the first comprised of purely ambient data before the FO, the second contained the FO, and the third was purely ambient data after the FO. As seen in Table I, both sets of ambient data estimated the major interarea mode to be about 0.2 Hz with damping greater than 10%, which agrees with the analyses in [8]. During the FO, however, the mode meter is exceptionally biased as it tries to model the FO as a system mode with 0.25 Hz and 0% damping.

The refined FO parameter estimates were used with the LS-ARMAX mode meter, which models the FO as system input $u[k]$, a cosine at the FO frequency with unity amplitude and zero phase [6]:

$$\hat{u}[k] = \cos(2\pi \frac{\hat{f}}{f_s} k) I_{\hat{\epsilon},\hat{\eta}}[k] \tag{10}$$

Initially, little improvement was seen. However, as noted in [8], the amplitude of the FO was time-varying. To account for this, the amplitude was re-estimated by applying the proposed algorithm to a sliding 20-minute window that advanced one sample at a time, calculating a new amplitude estimate each time. The other FO parameter estimates were virtually unchanged throughout this process and retained their aforementioned values.

A reconstructed estimate of the FO using the time-varying amplitude estimate is shown in Fig. 6, where very good agreement is seen. Indeed, this was used to estimate the 10.8

TABLE I
JANUARY 11, 2019 EI FO EVENT: MODE ESTIMATES

	frequency	damping	
Prior to FO	0.2076 Hz	16.96 %	LS-ARMA
During FO	0.2493 Hz	0.387 %	LS-ARMA
	0.2218 Hz	**11.93 %**	**LS-ARMAX**
After the FO	0.1954 Hz	12.85 %	LS-ARMA

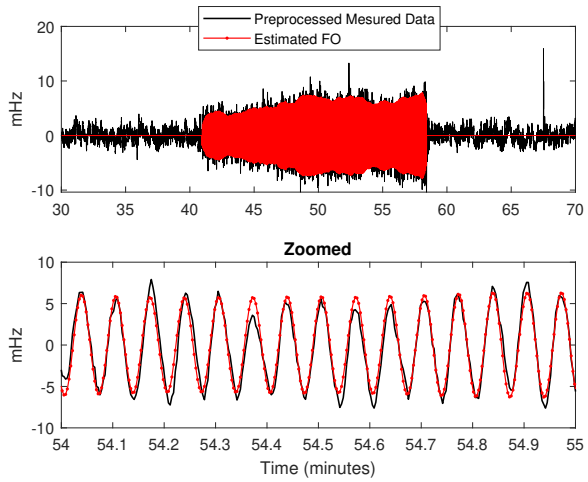

Fig. 6. Comparison of the estimated EI FO with the preprocessed measured data (top) with a zoomed view (bottom).

dB SNR condition. A new estimated input that contained the slowly varying amplitude was created

$$\hat{u}[k] = \hat{A}[k]\cos(2\pi\frac{\hat{f}}{f_s}k)I_{\hat{\epsilon},\hat{\eta}}[k] \tag{11}$$

and applied to the LS-ARMAX mode meter. The results, shown in bold in Table I, align nicely with the pre- and post-FO ambient data, suggesting the validity of the proposed method.

VI. CONCLUSIONS

This paper presents a method of estimating FO parameters from measured power system data. Through simulations it is shown that the refinement stage can result in estimators that are unbiased and reach the CRLB over a wide range of SNR. The algorithm was applied to an actual FO event, where the estimated FO parameters showed good agreement with the analysis of [8] and were shown to effectively correct the bias seen by an ambient mode meter - even in the presence of time-varying FO amplitude.

Future work includes a study of the convergence of the algorithm. In both the simulation and EI settings investigated here, it was found that convergence was mostly achieved at Q=2, with the occasional Monte Carlo trial converging at Q=3. A much more robust investigation into convergence is needed. Other future research topics include extending the work to address FOs that are nonstationary in both amplitude and frequency, as well as an extensive simulation study of the effects of the algorithm on mode meter performance. Finally, for the purpose of mode meter bias removal, conceptualizing FOs as exogenous power system inputs is fine. However, there is still much to be done in the area of analyzing the physical sources of FOs and their appropriate corrective measures.

REFERENCES

[1] C. Wang, C. Mishra, K. D. Jones, R. M. Gardner, and L. Vanfretti, "Identifying oscillations injected by inverter-based solar energy sources," in *2022 IEEE Power & Energy Society General Meeting (PESGM)*, 2022, pp. 1–5.

[2] L. Vanfretti, S. Bengtsson, V. S. Perić, and J. O. Gjerde, "Effects of forced oscillations in power system damping estimation," in *Applied Measurements for Power Systems (AMPS), 2012 IEEE International Workshop on*. IEEE, 2012, pp. 1–6.

[3] J. Follum, J. W. Pierre, and R. Martin, "Simultaneous estimation of electromechanical modes and forced oscillations," *IEEE Transactions on Power Systems*, vol. 32, no. 5, pp. 3958–3967, Sept 2017.

[4] U. Agrawal, J. Follum, J. W. Pierre, and D. Duan, "Electromechanical mode estimation in the presence of periodic forced oscillations," *IEEE Transactions on Power Systems*, 2018.

[5] L. Dosiek, U. Agrawal, J. Follum, J. W. Pierre, and D. J. Trudnowski, "Analysis of power system mode meters under various oscillatory conditions," in *2018 IEEE International Conference on Probabilistic Methods Applied to Power Systems (PMAPS)*, 2018, pp. 1–6.

[6] L. Dosiek, "Strategies for addressing forced oscillations with the multi-channel least squares mode meter," in *2019 IEEE Power Energy Society General Meeting (PESGM)*, 2019, pp. 1–5.

[7] ——, "The effects of forced oscillation frequency estimation error on the ls-arma+s mode meter," *IEEE Transactions on Power Systems*, vol. 35, no. 2, pp. 1650–1652, 2020.

[8] A. Alam et al., "Eastern interconnection oscillation disturbance januarry 11, 2019 forced oscillation event," North American Electric Reliability Corporation (NERC), Tech. Rep., December 2019.

[9] S. Djukanović, "An accurate method for frequency estimation of a real sinusoid," *IEEE Signal Processing Letters*, vol. 23, no. 7, pp. 915–918, 2016.

[10] L. Dosiek and S. Hosur, "Improved time-localization of power system forced oscillations using changepoint detection," in *2022 IEEE Power & Energy Society General Meeting (PESGM)*, 2022, pp. 01–05.

[11] S. M. Kay, *Fundamentals of statistical signal processing: estimation theory*. Prentice-Hall, Inc., 1993, vol. 1.

[12] L. Marple, "Computing the discrete-time analytic signal via fft," *IEEE Transactions on Signal Processing*, vol. 47, no. 9, pp. 2600–2603, 1999.

[13] E. Aboutanios and B. Mulgrew, "Iterative frequency estimation by interpolation on fourier coefficients," *IEEE Transactions on Signal Processing*, vol. 53, no. 4, pp. 1237–1242, 2005.

[14] C. Candan, "Analysis and further improvement of fine resolution frequency estimation method from three dft samples," *IEEE Signal Processing Letters*, vol. 20, no. 9, pp. 913–916, 2013.

[15] J. Follum and J. Pierre, "Time-localization of forced oscillations in power systems," in *Power & Energy Society General Meeting, 2015 IEEE*. IEEE, 2015, pp. 1–5.

[16] S. M. Kay, *Fundamentals of statistical signal processing: detection theory*. Prentice-Hall, Inc., 1998, vol. 2.

[17] Z. Xu and J. W. Pierre, "Initial results for cramer-rao lower bound for forced oscillations in power systems," in *2021 North American Power Symposium (NAPS)*, 2021, pp. 1–5.

[18] Z. Xu, J. W. Pierre, R. Elliott, D. Schoenwald, F. Wilches-Bernal, and B. Pierre, "Cramer-rao lower bound for forced oscillations under multi-channel power systems measurements," in *2022 17th International Conference on Probabilistic Methods Applied to Power Systems (PMAPS)*, 2022, pp. 1–6.

[19] J. Follum and J. W. Pierre, "Detection of periodic forced oscillations in power systems," *IEEE Transactions on Power Systems*, vol. 31, no. 3, pp. 2423–2433, 2016.

[20] L. Dosiek, "On the cramer–rao bound of power system electromechanical mode meters," *IEEE Transactions on Power Systems*, vol. 34, no. 6, pp. 4674–4683, 2019.

[21] D. Trudnowski, D. Kosterev, and J. Undrill, "PDCI damping control analysis for the western north american power system," in *2013 IEEE Power Energy Society General Meeting*, July 2013, pp. 1–5.